Journal of
Composites Science

MDPI

Article

The Capillary Suspension Concept Is Used to Obtain Polymer-Free Particle Contacts Enhancing Conductivity of Highly Filled Polymer Composites

Katrin Dyhr *, Karim Abdel Aal, Anna-Maria Steck and Norbert Willenbacher

Institute of Mechanical Process Engineering and Mechanics, Karlsruhe Institute of Technology, 76131 Karlsruhe, Germany; norbert.willenbacher@kit.edu (N.W.)
* Correspondence: katrin.dyhr@kit.edu

Abstract

Usually, particle morphology and surface treatment are adjusted to achieve high conductivity in highly filled conductive polymer composites. Here, we demonstrate that this key property can be further improved by keeping the particle contact regions free of polymer using an extension of the capillary suspension concept. If the secondary liquid is chosen such that it remains in the contact areas between conductive particles during solidification of the polymer phase, then the composite conductivity substantially increases. For both a thermoset and a thermoplastic model system including 40 vol.% silver particles in the paste, the conductivity was more than doubled compared to the respective binary system, reaching conductivity values up to $(4.3 \pm 0.2) \times 10^6$ Sm^{-1}. SEM images clearly show the polymer-free contact regions in samples with enhanced conductivity. However, conductivity only increases if the secondary fluid is removed after solidification of the polymer phase. Thus, the capillary suspension concept can be used for a controlled modification of particle–particle contacts and represents a generic, viable strategy for enhancing conductivity in highly filled polymer composites. The concept helps to save precious (silver) resources and may find application in various fields of printed electronics, e.g., metallization of thermosensitive solar cells.

Keywords: low temperature curing; printed electronics; conductivity enhancement; polymeric binders; solar cell metallization

1. Introduction

Electronic products infiltrate every aspect of our life today, from energy generation and storage, communication technology, industrial automation to data processing in administration and science, and even medical applications. The social relevance of electronics can be quantified by the amount of electronic waste generated [1]. The global annual per capita consumption of electronics was 7.8 kg in 2022, while the figures in Europe, Oceania, and the Americas are significantly above this average with values from 14.1 kg to 17.6 kg [2]. Several printing processes are used in mass production of printed electronics. These include screen printing, dispensing, stencil printing, direct ink writing, jetting and other less common methods such as pattern transfer printing [3–5]. What all these processes have in common is that the conductive material must be prepared as a paste suitable for the respective application process [1,3,6,7].

Depending on the application, two classes of printable pastes can be distinguished. On the one hand, there are pastes that sinter at high temperatures, such as those used in

Academic Editor: Fubin Luo

Received: 26 May 2026
Revised: 20 June 2026
Accepted: 23 June 2026
Published: 26 June 2026

manufacturing of solar cells [8–10]. On the other hand, temperature-sensitive applications such as heterojunction or perovskite tandem solar cells, or printed electronic products on temperature-sensitive, flexible polymeric substrates require pastes that cure at low temperatures well below 250 or even 150 °C [11,12]. These pastes contain a polymeric binder, which ensures cohesion of the printed structure and its adhesion to the substrate [13]. Besides that difference, low temperature curing printing pastes typically contain conductive fillers, additives and solvents similar to high temperature pastes [11].

The polymeric binders in low temperature curing pastes and electrically conductive adhesives (ECAs) for printed electronics can be divided into two groups: reactive thermosetting systems such as epoxy or acrylic resins, and thermoplastic systems such as polyols, polyamides, or polyurethanes [14]. Depending on the application, either thermosetting systems with their higher strength, low shrinkage and temperature stability [15] or thermoplastic systems which can be fluidized again, and offer a wide range of flexibility [16] may be more suitable. Silver is often used as a conductive material due to its high electrical conductivity ($\kappa \approx 6.3 \times 10^7$ Sm^{-1}). Alternatives include copper, aluminum, or graphite [17,18]. Due to the intensive use of silver in all areas of printed electronics, particularly in photovoltaics, shortages are to be expected. Hallam et al. conclude that in a business-as-usual scenario, around 85 to 98 percent of global silver reserves would be committed to photovoltaics alone by 2050 [19]. The rising silver prices on the stock markets in recent years reflect this trend towards a scarcity of the precious metal, which is manifested in a six-year deficit in the silver supply [20].

To reduce silver usage and maintain a high conductivity, numerous strategies have been developed. It has been demonstrated that the morphology of conductive particles (flake-shaped or spherical, micro- or nanoscale) has a decisive influence on the conductivity of the corresponding printed as well as cured or dried structures. The critical concentration to achieve percolation can be reduced using filler particles, with higher surface area [21]. A broad compared to a narrow particle size distribution also resulted in a lower percolation threshold [22]. While large flake-shaped particles show high contact areas and thus improve conductivity [23], nanoscale particles promote sintering even at low temperatures [24]. On the other hand, organic surface layers introduced to disperse and stabilize the particles in the binder phase may prevent sintering and due to its insulating properties deteriorate electrical conductivity [24]. This highlights the importance of particle stabilizer type and amount on the resulting conductivity of the finally printed feature [25]. These stabilizers can be of polymeric nature such as, for example, polyvinylpyrrolidone (PVP) or small molecules like alkanethiols, alkylamines and carboxylic acids and it is important to use the agent with suitable decomposition temperatures to maximize the sintering effect [26]. A completely different approach is to increase conductivity by adding inert fillers or gas bubbles, creating excluded volume thereby facilitating the formation of conductive pathways around these non-conductive regions and thus reducing the percolation threshold [27–30]. Inert fillers with a conductive coating layer are a special case of this concept [31]. Furthermore, bicontinuous polymer structures can be used to significantly lower the percolation threshold and thereby influence electrical conductivity [32].

Although these methods all bring significant improvements, they essentially follow the same basic approach, in which particles are dispersed in a carrier medium, often also termed vehicle. Further improvements can be achieved by adopting a fundamentally different approach that utilizes the principle of capillary suspensions instead of two-phase systems. Capillary suspensions are ternary particle–liquid–liquid systems [33]. The addition of small amounts of a secondary liquid immiscible with the continuous phase induces the formation of a continuous particle network due to capillary forces. The strength of the particle network depends on the interfacial tension between both liquids, the contact angle

of the secondary fluid on the particles, and the amount of secondary liquid relative to the particle volume fraction [33]. It is not necessary that the secondary liquid preferentially wets the particles [33], and the network that forms allows the flow properties and storage stability of a suspension to be adjusted without the need for additional additives. Beyond that, formulations based on capillary suspensions enable a shift in the percolation threshold for conductive, printable metal-polymer composites. For conductive elastomers, the capillary suspension concept was used to significantly shift the percolation threshold while simultaneously achieving improved mechanical properties, particularly a higher durability during cyclic loading [34,35]. Capillary suspensions have also been used to formulate electrically conductive adhesives (ECAs) [31] with below 4 vol% silver content while still meeting the specifications for shingled solar cell interconnection in terms of volume and contact resistivity as well as mechanical strength in the cured and sufficient shelf-life and printing properties in the uncured state [31]. On the other hand, no improvement in conductivity due to the capillary suspension effect has yet been demonstrated in polymer-metal composites with filler content clearly exceeding the percolation threshold [35]. One reason is that, even without strong attractive forces among particles, there are plenty of particle contact points in the material simply due to geometrical constraints.

So far it has been demonstrated that the capillary suspension concept can be used to increase conductivity in composites of polymer and conductive fillers at low and intermediate particle loadings due to a shift in the percolation threshold. In the work presented here, we demonstrate that this concept can also be used to enhance the conductivity of concentrated systems well above the percolation threshold with an already large number of particle contacts due to geometrical constraints. To achieve this, the secondary liquid is chosen such that it remains in the particle contact region during solidification or curing of the polymer included in the primary phase [36]. The secondary liquid thus prevents the polymer from entering into the contact regions. After solidification, however, it should leave the sample so that it does not act as an insulating layer in the particle contact areas. Accordingly, the secondary liquid should have a higher boiling point and/or lower vapor pressure than the solvent in the primary fluid. The effectiveness of this novel approach is demonstrated in detail using a thermosetting system systematically modified using secondary liquids with boiling points below, equal, and above that of the primary phase. The study examines how this affects the conductivity of the solidified material and whether the increase in conductivity is indeed attributable to polymer-free contact points. The general applicability of the concept also to thermoplastic systems is then demonstrated using the most effective secondary liquid from the first part of the investigation. Commercially available, nearly monodisperse, spherical silver particles have been used for this proof of concept. A transfer to other particle shapes should be addressed in future research.

2. Materials and Methods

A flowchart summarizing the workflow of sample preparation and characterization is shown in Figure 1.

2.1. Paste Preparation

For the model systems investigated here, the primary (continuous) phase consists of the solvent benzyl alcohol (Carl Roth GmbH + Co. KG, Karlsruhe, Germany) and a specified mass fraction of epoxy resin (EP-Gießharz wasserklar, R&G Faserverbundwerkstoffe GmbH, Waldenbuch, Germany) as binder. For the thermoplastic system, the polyvinylacetate with a molecular weight of 170,000 g/mol (Thermo Fisher Scientific Inc., Waltham, MA, USA) was used here instead of the epoxy resin. Figure 2 summarizes the characteristics of the utilized particles. Spherical silver particles (K-7418P, Metalor Tech-

nologies SA, Marin-Epagnier, Switzerland) which exhibit a nearly monodisperse particle size distribution with a mean particle size of $x_{50,3} = 1.43 \pm 0.01$ µm were used as conductive filler. The equivalent diameter of the particles was characterized using a HELOS H0309 laser diffraction instrument (Sympatec GmbH, Clausthal-Zellerfeld, Germany). The particles are hydrophobically modified. The amount of the dispersant was determined using TGA analysis (TGA 5500, Waters GmbH, Eschborn, Germany).

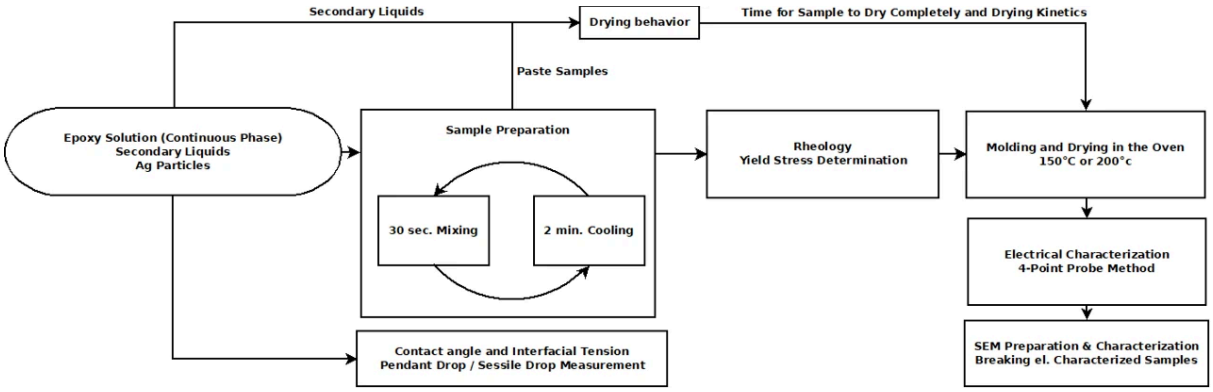

Figure 1. Flowchart depicting the workflow of sample preparation and characterization.

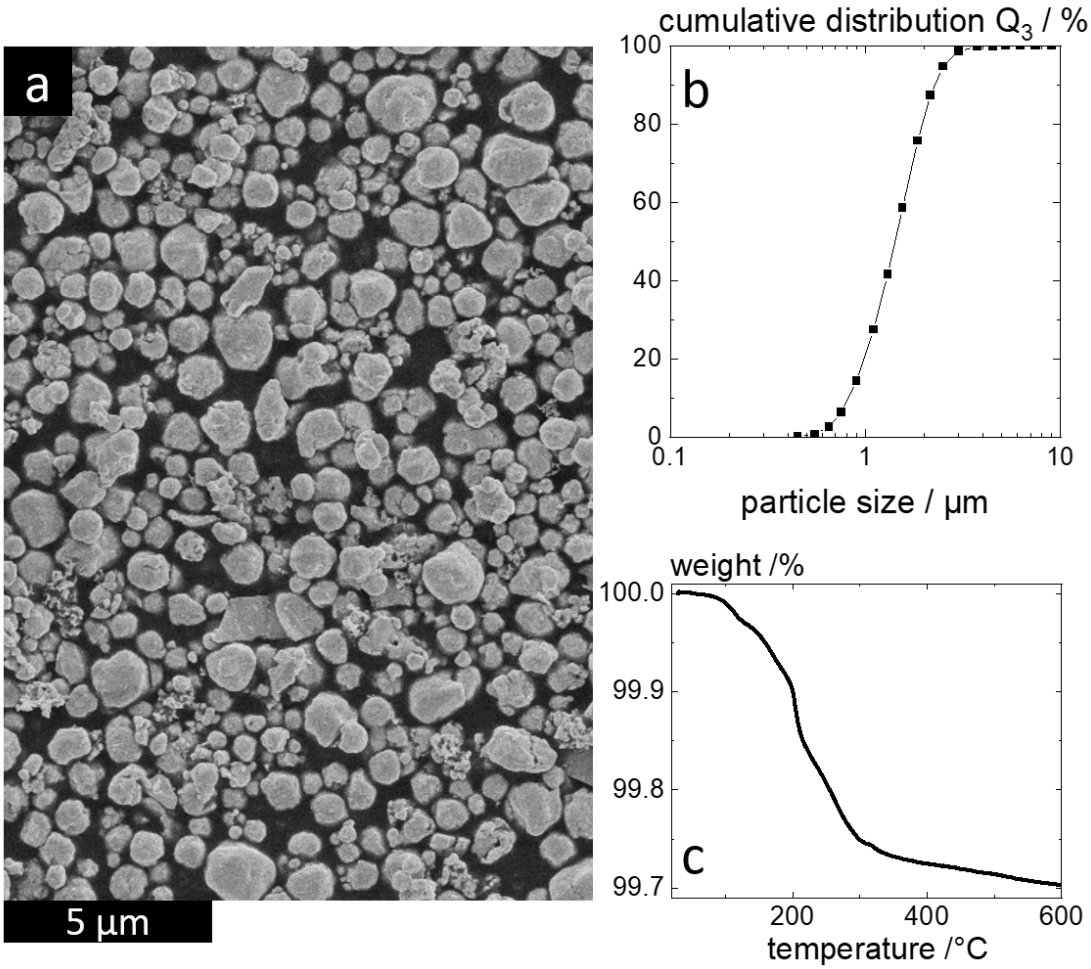

Figure 2. Characterization of silver particles K-7418P (Metalor): (**a**) SEM image providing an overview of shape and size variation, (**b**) equivalent sphere particle size distribution as obtained from Fraunhofer diffraction, (**c**) thermogravimetric particle analysis characterizing the amount of organic surface layer.

Proprietary aliphatic hydrocarbon mixtures were employed as secondary liquids. Three mixtures with similar chemical composition but different chain lengths were selected, resulting in a low boiling temperature range (135 to 180 °C), a medium boiling temperature range (179 to 210 °C), and a high boiling temperature range (255 to 290 °C). For simplicity, these mixtures are referred to as low boiling, medium boiling, and high boiling in the following sections.

After adding all components, the sample was mixed four times for 30 s at 2000 rpm (SpeedMixer DAC 150.1 FVZ, Hauschild & Co. KG, Hamm, Germany). In between the mixing steps, the sample was allowed to rest for at least 2 min to prevent undesired heating caused by mixing.

2.2. Paste Characterization

2.2.1. Yield Stress Determination

A rotational rheometer equipped with a vane geometry (Physica MCR 501, Anton Paar GmbH, Graz, Austria) was used to determine the yield stress σ_y of the prepared samples at 25 °C. A rectangular base was used to prevent slippage and ensure that the measurement was not compromised. The applied shear stress was increased stepwise from 0.1 to 1000 Pa or from 1 to 10,000 Pa, depending on the expected yield stress, using 81 logarithmically spaced steps with a duration of 10 s each. The resulting deformation was recorded and plotted in a double-logarithmic strain–stress diagram. For yield stress fluids, the γ vs. σ curves typically exhibit an initial branch with a slope of 1, corresponding to the elastic response regime at $\sigma < \sigma_y$, followed by a pronounced kink and a subsequent branch with a substantially higher slope. The yield stress was determined using the tangent intersection method [37,38]. Each sample was measured three times. Mean values were calculated from the triplicate measurements. The reported error represents the combined uncertainty, including the standard deviation of the measurements and the estimated experimental uncertainty arising from sample preparation.

2.2.2. Interfacial Tension and Contact Angle

The pendant drop method was applied to determine the interfacial tension. A drop of the continuous phase consisting of solvent with varying amounts of epoxy resin was dispensed using a hollow needle (diameter d = 1.82 mm) into a glass cuvette filled with the different secondary liquids. At least 12 measurements were taken for each secondary liquid–continuous phase combination.

Contact angle data were determined using the sessile drop method. Silver plates were prepared by pressing 3 g of silver particles at 400 bar for 5 min. The formation of the particle network in capillary suspensions is related to the three-phase contact angle of the secondary liquid on the particles covered by the continuous phase liquid. Measuring this quantity is not feasible here, since the secondary liquid wets the silver particles very well and penetrates into the pores of the plate made from these particles. Instead, we have measured the three-phase contact angle of the continuous phase liquid on the silver plate covered by the secondary liquids. For these measurements the plate was immersed in the secondary liquid, and at least six 1 µL droplets of epoxy solution were deposited onto the plate surface. The measurement setup and procedures for determining the contact angle and interfacial tension were carried out in accordance to DIN EN ISO 19403 [39].

Interfacial tension and contact angle values were calculated from the measurement data using the commercial software Drop Shape Analysis (DSA version 1.90.0.14, Krüss GmbH, Hamburg, Germany); typical drop shapes are shown in Figure 3.

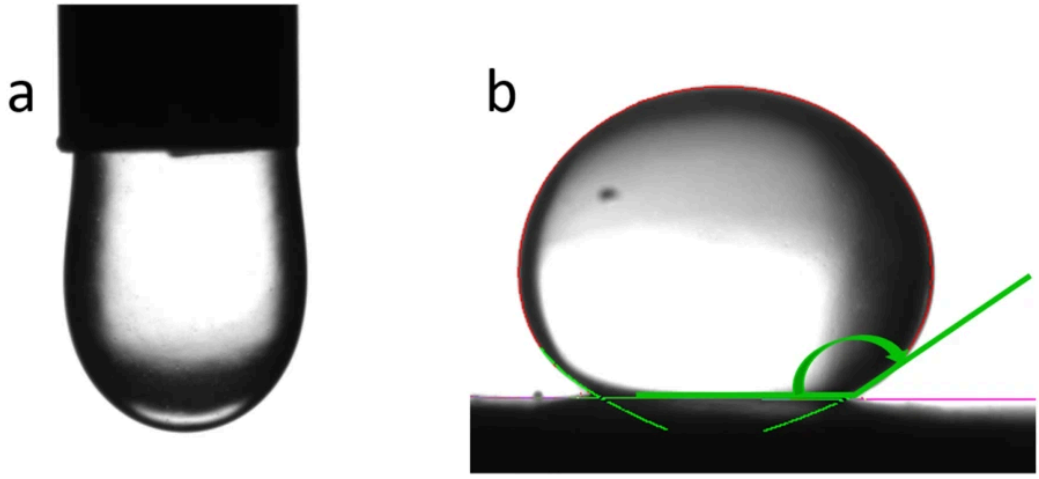

Figure 3. Examples of droplet evaluation: (**a**) pendant drop for interfacial tension measurement, (**b**) sessile drop for contact angle determination.

2.2.3. Drying Behavior

A stencil with a width of 4 mm and a thickness of 100 µm was used to apply three 70 mm long lines on a glass slide. The wet layer height corresponds to the thickness of the used stencil. The samples were placed in a drying scale HX204 Halogen Moisture Analyzer (Mettler Toledo, Greifensee, Switzerland) using a temperature of 150 °C and a total drying time of 15 min sufficient to remove all solvents. The initial drying rate in the surface-controlled regime was determined using a linear fit. For each characterized sample, three measurements were conducted and the mean value and standard deviation were calculated.

2.3. Characterization of the Dry Polymer Composite

2.3.1. Electrical and Mechanical Characterization

Two samples for each paste were prepared according to 2.2.3 and dried in an oven at 150 °C or 200 °C for 10 min. Four measurements per line strip were taken using a four-point-probe measurement with a 2450 SourceMeter (Keithley, Cleveland, OH, USA) at a current of 10, 50 and 100 mA. The mean value and standard deviation were calculated. Using the same drying conditions, the samples were prepared for Shore A hardness tests, which were conducted according to ASTM D2240 [40].

2.3.2. SEM Imaging

Samples for imaging were prepared using the same cured samples on glass slides as used for electrical characterization. To create a straight fracture edge, the samples were scored and broken along the crack. After sputtering, scanning electron microscopy (SEM) was performed using a Phenom Pharos G2 (Thermo Fisher Scientific Inc., Waltham, MA, USA). For each polymer content, 20 randomly distributed images were taken, corresponding to 5 images per sample.

3. Results and Discussion

3.1. Macrostructure of Particle Network

In capillary suspensions, the yield stress typically rises upon addition of the secondary liquid compared to the corresponding binary suspension in a characteristic manner [33]. This behavior is therefore often used as an indicator of the formation of the capillary particle network. Thus, in Section 3.1.1, the yield stress is used to characterize the particle network

in the paste, while in Section 3.1.2, the preservation of the network in the dry and cured composite is evaluated using SEM images.

3.1.1. Characterization in Paste Composition

Figure 4a shows the yield stress as a function of the ratio of secondary liquid to particle volume fraction for a continuous phase consisting of a 40 wt.% epoxy solution and three secondary liquid types with different boiling ranges. To show the effect of capillary suspensions on creating polymer-free particle contact zones, all other parameters were kept constant and a typical particle loading of 40 vol% was selected.

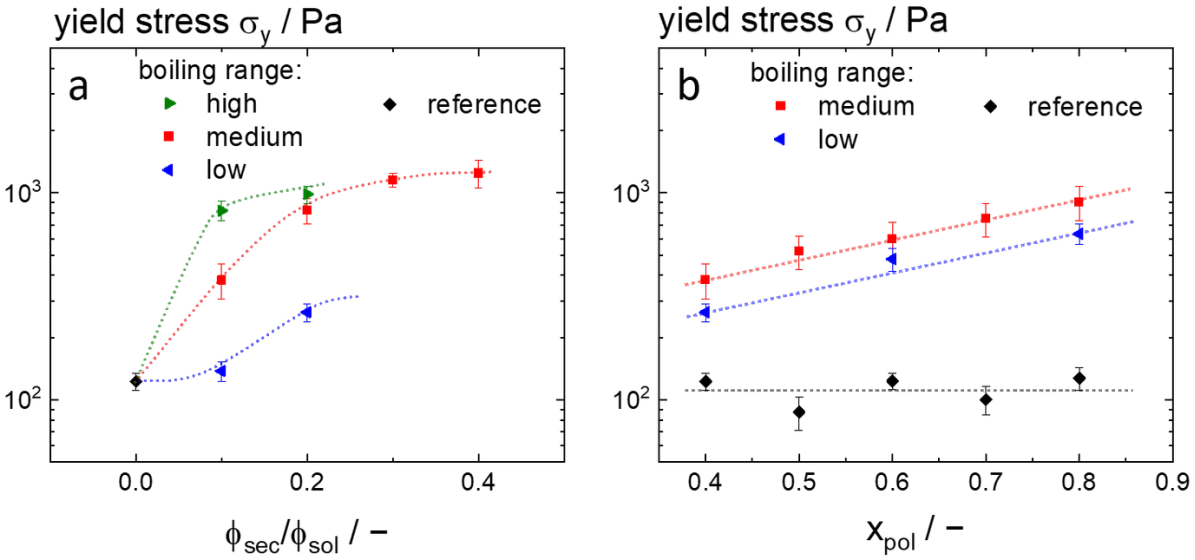

Figure 4. Yield stress of capillary suspensions including 40 vol% spherical silver particles as conductive fillers and a solution of epoxy resin in benzyl alcohol as primary liquid phase (**a**) as a function of secondary liquid to solid fraction for secondary liquids with varying boiling ranges and 40 wt.% epoxy solution as continuous phase and (**b**) as a function of the epoxy weight fraction (x_{pol}) in the continuous phase for samples without a secondary liquid (black), a medium boiling secondary liquid with ϕ_{sec}/ϕ_{sol} = 0.1 (red) and a low boiling secondary liquid with ϕ_{sec}/ϕ_{sol} = 0.2 (blue); lines are to guide the eye.

Samples including the medium boiling secondary liquid (red) were characterized over a broad range of ϕ_{sec}/ϕ_{sol} and show the behavior expected for capillary suspensions [33] mentioned above. As the proportion of secondary liquid increases, the yield stress σ_y rises sharply until it reaches a plateau. Qualitatively, a similar behavior is found for the other two secondary liquids, for the high boiling secondary liquid the plateau in σ_y seems to be reached at lower ϕ_{sec}/ϕ_{sol} and for the low boiling secondary fluid the increase in σ_y apparently sets in at higher ϕ_{sec}/ϕ_{sol}. As expected [33], at a given ratio ϕ_{sec}/ϕ_{sol}, the increase in σ_y is more pronounced at a higher interfacial tension among both liquid phases; the corresponding data are listed in Table 1.

Table 1. Interfacial properties of 40 wt.% epoxy solution and secondary liquids with different boiling ranges.

Boiling Range	Low: 135–180 °C	Medium: 179–210 °C	High: 255–290 °C
interfacial tension/mN/m	0.89 ± 0.03	2.72 ± 0.03	3.42 ± 0.03
normalized by lowest value	1	3.05 ± 0.10	3.83 ± 0.13
three-phase contact angle of 40 wt % epoxy solution in sec. liquid/°	130 ± 8	131 ± 6	141 ± 5

In addition to interfacial tension, the wetting properties between both liquids and the particle surface have a significant influence on structure formation and flow characteristics of capillary suspensions [33]. Therefore, the wetting behavior in the three-phase system was examined. When attempting to measure the contact angle of secondary fluid droplets on the plate pressed from the silver particles, the secondary liquid was absorbed into the plate due to residual porosity. This behavior indicates that the secondary liquid wets the particles very well and that a pendular state capillary suspension forms. To further support this conclusion, the three-phase contact angle of a 40 wt.% epoxy solution was measured in the presence of the secondary liquids. Table 1 shows that the epoxy solution exhibits a high contact angle irrespective of the secondary liquid surrounding it. Therefore, we conclude that the secondary fluid preferentially wets the particles compared to the primary fluid, i.e., a pendular state capillary suspension forms in the ternary system investigated here. Figure 4b shows the yield stress as a function of polymer content in the continuous phase. Exemplarily, the two-phase system is compared to the three-phase system with the medium boiling secondary liquid at ϕ_{sec}/ϕ_{sol} = 0.1 and the low boiling secondary liquid at ϕ_{sec}/ϕ_{sol} = 0.2. In the absence of a secondary liquid, the polymer fraction has no significant influence on the yield stress. The values vary between 109 ± 20 Pa, which essentially corresponds to the experimental uncertainty. In contrast, when a secondary liquid is present, the yield stress increases significantly with increasing polymer content. For the low boiling secondary liquid, σ_y rises from 264 ± 26 Pa to 634 ± 71 Pa. This 2.4 ± 0.4 increase in yield stress corresponds to the increase in interfacial tension as can be seen from the normalized data shown in Table 2. For the medium boiling secondary liquid, σ_y increases from 380 ± 73 Pa to 903 ± 170 Pa. As can be seen from the data in Table 2, this represents a stronger increase than would be expected based solely on the weak rise in interfacial tension. This is an indication that other factors, such as a change in droplet breakup during mixing due to the increase in viscosity of the continuous phase, may also play a role here.

Table 2. Interfacial tension between epoxy solutions with different resin contents in low boiling and medium boiling secondary liquid, respectively.

	Epoxy Fraction x_{pol}/wt %	**50**	**60**	**70**	**80**
Low boiling	interfacial tension/mN/m	1.27 ± 0.01	1.55 ± 0.03	1.89 ± 0.04	2.19 ± 0.04
	normalized by lowest value	1.42 ± 0.05	1.74 ± 0.06	2.13 ± 0.08	2.46 ± 0.09
Medium boiling	interfacial tension/mN/m	3.19 ± 0.02	3.57 ± 0.01	4.04 ± 0.02	4.30 ± 0.01
	normalized by lowest value	1.17 ± 0.01	1.31 ± 0.02	1.49 ± 0.02	1.58 ± 0.02

Overall, it is evident that a capillary network forms for all investigated secondary liquids and polymer contents. However, for the low boiling secondary liquid, ϕ_{sec}/ϕ_{sol} must exceed 0.1 to facilitate stable network formation, presumably due to partial miscibility of this low molecular weight hydrocarbon mixture and the need to saturate the continuous phase prior to network formation.

The drying behavior of the pastes was characterized and the time required for the films to dry completely was well below the total drying time employed to create films for conductivity measurements. It appeared to be roughly independent of paste composition (polymer content, presence and boiling temperature of secondary fluid). Differences occurred, however, in the initial drying rate; the corresponding data are summarized in Table 3.

Table 3. Initial drying rate during film formation from pastes with different types of secondary liquid and different epoxy fractions in the primary liquid. The silver fraction in the wet pastes was always 40 vol%, the secondary fluid to particle volume fraction was ϕ_{sec}/ϕ_{sol} = 0.1 in all cases. The initial film thickness was 100 µm.

Boiling Range of Sec. Liquid	Epoxy Fraction x_{pol}/wt.%	Initial Drying Rate/mg/s
no sec. liquid	40	0.38 ± 0.01
low	40	0.39 ± 0.02
medium	40	0.41 ± 0.02
high	40	0.39 ± 0.02
medium	60	0.22 ± 0.04
medium	80	0.10 ± 0.01

The initial drying rate of the capillary suspension type for ternary pastes is the same as for the binary reference paste, irrespective of the boiling range of the secondary liquid. In contrast, earlier work on polymer-free suspension showed that the particle network controlled by capillary forces preserved the open pores in the sample and accelerated sample drying [41]. This suggests that the drying rate here is mainly controlled by the polymer films in the pores between the particles serving as diffusion barrier. This is further supported by the significant decrease in initial drying rate with increasing polymer content in the primary liquid. Furthermore, the pure solvent drying behavior was characterized at 150 °C for 10 min. The high boiling secondary liquid exhibits an evaporation rate of 0.24 mg/s, which is significantly lower than that of the medium boiling liquid (4.5 mg/s) and also lower than that of the vehicle solvent (0.55 mg/s). Since 150 °C is in the boiling range of the low boiling secondary liquid, its evaporation speed could not be determined.

To determine whether the curing kinetics of the epoxy resin are affected by the secondary liquid, DSC measurements were carried out. No shift in the exothermic curing peak was observed. Both the reference paste and the capillary suspensions with all three secondary liquids were cured in the temperature range of 130–155 °C, with a peak at 143.9 ± 0.5 °C. No changes in the mechanical strength of the composites were detected, as confirmed by Shore A hardness tests conducted according to ASTM D2240, which yielded values of 92 ± 2 for all samples. Next, the microstructure and electrical conductivity of the cured composites will be discussed.

3.1.2. Overall Structure of Cured Composites from Binary and Ternary Pastes as Characterized by SEM

Sample preparation methods for SEM imaging may deteriorate the microstructure of a polymer composite, particularly the contact regions between particles. Mechanical grinding and polishing, for example, may smear the polymer into the particle–particle contact points and thereby alter the native structure of the network. To minimize preparation-induced artifacts and to preserve both the particle network structure and the polymer distribution around the particles, fracture surfaces were chosen for characterization. Epoxy resin used here fractures in a brittle manner, such that the internal structure of the sample is hardly affected by the fracture process. Figure 5 illustrates the resulting overall structure of the samples prepared according to this method. Both the films made from binary and ternary capillary suspension-type pastes exhibit an open porous structure (black regions in the SEM images).The particle/polymer mixture does not collapse to a dense film upon evaporation of the solvent. Particularly at the lowest concentration, the polymer does not fill the voids between the particles as can be seen in the first line of Figure 5. The open porosity decreases as the polymer content increases and the area of the featureless regions representing the polymer increases. Moreover, the films made from binary pastes show numerous residuals of large gas bubbles. In these samples, collapse of the particle network during drying is

more pronounced and the smaller capillaries between the particles are partly closed by polymer films locally preventing solvent evaporation and leading to the formation of large round voids. The extent of this void formation increases with increasing polymer content, indicating a stronger restriction of solvent transport at higher polymer fractions.

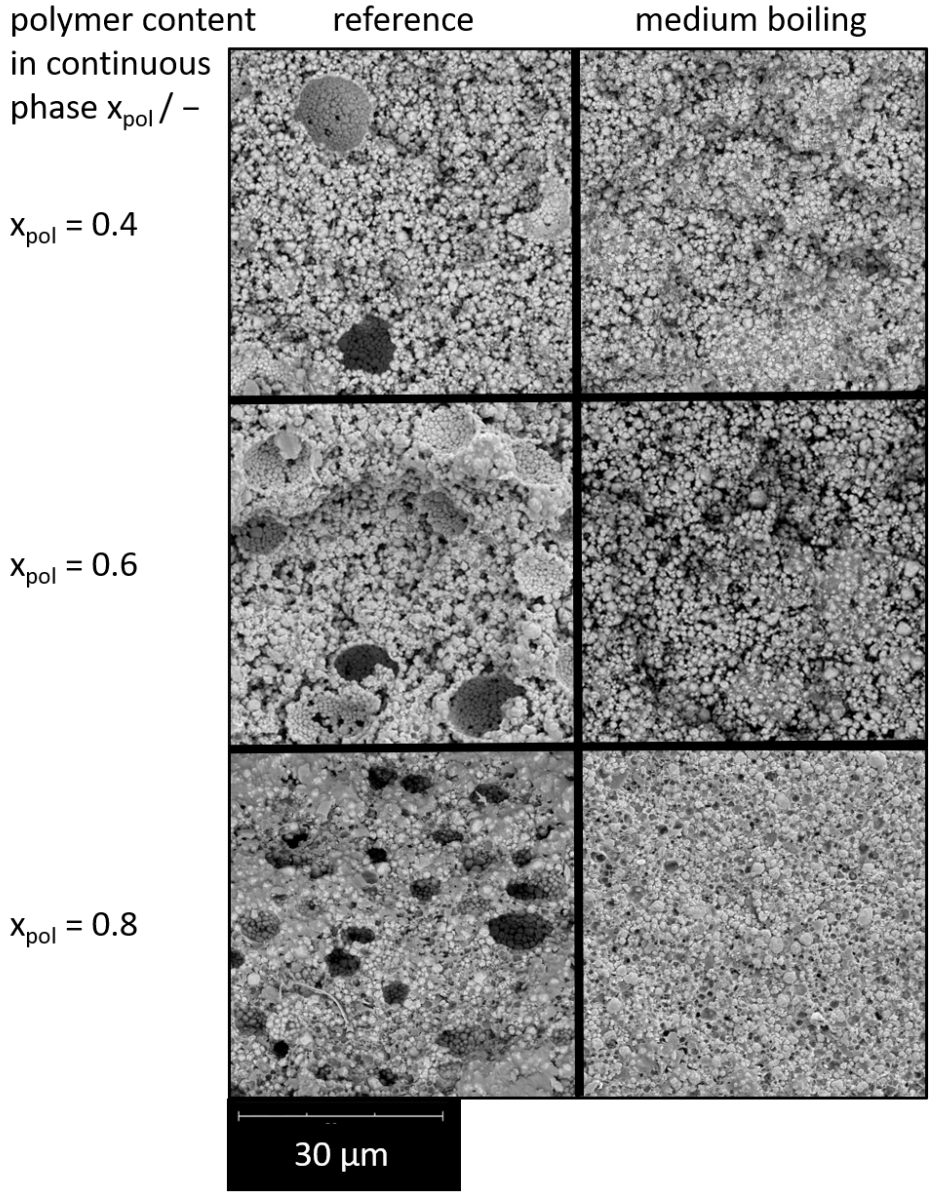

Figure 5. SEM image of fractured samples without secondary liquid (**left**) and with medium boiling secondary liquid at ϕ_{sec}/ϕ_{sol} = 0.1 (**right**). The particle content in the wet paste was 40 vol% in all cases and the resin content in the continuous phase (x_{pol}) was set to 40, 60, and 80 wt.%.

Such voids do not occur in the films made from ternary pastes. This suggests that the porous structure of the particle network controlled by capillary forces is preserved during drying as observed earlier [42] and does not allow for the formation of closed polymer films, thus facilitating solvent escape.

3.2. Electrical Conductivity of Polymer Composites

Numerous strategies have been developed to enhance conductivity in highly filled polymer composites at a given silver content, including optimization of particle morphology and size distribution, control of stabilizers and their decomposition, as well as the use of

inert fillers, gas bubbles, or bi-continuous structures to lower the percolation threshold. Building on this, we investigate whether capillary suspensions represent a viable additional approach to further improve conductivity by promoting the formation of polymer-free contact regions between particles. Figure 6(a.1,a.2) depicts the electrical conductivity as a function of the ratio of secondary liquid to particle volume fraction for the three secondary liquids with different boiling ranges. The boiling range of the medium boiling liquid starts at 179 °C and ends at 210 °C, i.e., in the range of the boiling point of 205 °C of the benzyl alcohol in the primary continuous phase, whereas the boiling range of the high boiling liquid mixture commences at approximately 50 °C above that value. Data were collected at two different drying temperatures: 150 °C and 200 °C, well below and close to the boiling point of the benzyl alcohol in the primary continuous phase.

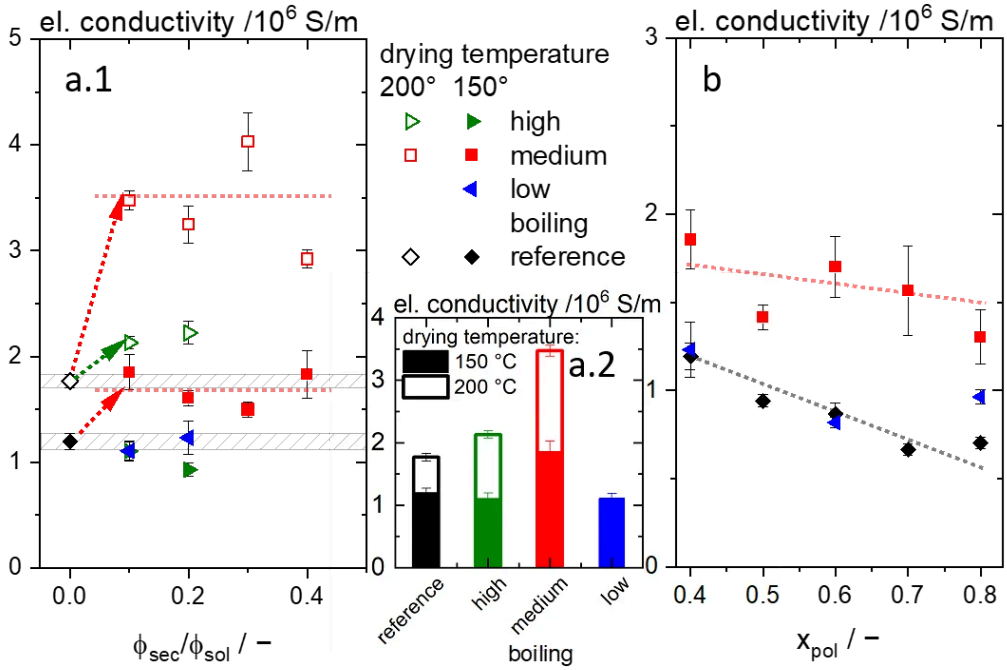

Figure 6. Electrical conductivity of capillary suspensions including 40 vol% spherical silver particles and a solution of epoxy resin in benzyl alcohol as primary liquid (**a.1**) as a function of secondary liquid to particle volume fraction for secondary liquids of varying boiling ranges, using a 40 wt.% epoxy solution, dried at 150 °C for 10 min (closed symbols) and at 200 °C for 10 min (open symbols), (**a.2**) for varying boiling ranges at a fixed secondary liquid to particle volume fraction of 0.1; samples with 40 wt.% epoxy solution were dried at 150 °C (closed) and 200 °C (open) and (**b**) as a function of the epoxy content in the continuous phase (x_{pol}) for samples without a secondary liquid (black), a medium boiling secondary liquid with ϕ_{sec}/ϕ_{sol} = 0.1 (red) and a low boiling secondary liquid with ϕ_{sec}/ϕ_{sol} = 0.2 (blue); samples were also dried for 10 min at 150 °C; lines and arrows are to guide the eye. The underlined grey area indicates the conductivity of the reference sample without the addition of a secondary liquid.

All samples containing the medium boiling secondary liquid exhibit an increased electrical conductivity compared to the reference without secondary liquid. At 150 °C drying temperature, this increase is in the range of 25–55%, whereas at 200 °C drying temperature, the electrical conductivity roughly doubles compared to the reference. Overall, there is no distinct dependence of conductivity on ϕ_{sec}/ϕ_{sol}. We assume that the medium boiling secondary liquid remains in the particle–particle contact regions until the polymer is immobilized due to capillary forces although its boiling range starts below the boiling point of benzyl alcohol. Thus, these regions are kept free of polymer in the dry film, finally leading to a higher electrical conductivity. The absolute conductivity values achieved at

200 °C drying temperature are about twice as high as for the samples dried at 150 °C presumably due to faster solvent evaporation and more pronounced partial sintering of small silver particles.

In contrast, the high boiling secondary liquid does not lead to a remarkable increase in conductivity. At 150 °C drying temperature, the conductivity even seems to decrease at higher secondary liquid fractions, most likely due to incomplete removal of the secondary liquid acting as an electrically insulating phase. This hypothesis is further supported by the evaporation data presented in Section 3.1 and in line with earlier investigations confirming that due to capillary the secondary liquid in capillary suspensions can be retained during drying, even if the temperature exceeds the boiling point [42].

At 200 °C drying temperature, the secondary liquid seems to be removed completely and a 26 ± 5% increase in electrical conductivity is found for $\phi_{sec}/\phi_{sol} = 0.2$. This increase is much less than observed for the medium boiling secondary liquid presumably because the slower removal of the high boiling liquid curtails the partial sintering of silver particles.

For the films made from pastes including the low boiling secondary fluid, no significant difference in electrical conductivity of the dry film was found even for the sample with $\phi_{sec}/\phi_{sol} = 0.2$, thereby clearly forming a capillary suspension in the wet state. We attribute this to the fast removal of the secondary liquid during drying, allowing the polymer to penetrate the particle–particle contact regions.

Figure 6b shows the electrical conductivity as a function of polymer content in the continuous phase of the wet paste for samples made from pastes including the medium boiling secondary liquid ($\phi_{sec}/\phi_{sol} = 0.1$) and from reference pastes without secondary liquid. Obviously, the conductivity decreases with increasing polymer content as expected, since more and more particle contacts are covered by the polymer. The decrease, however, is much weaker for the films made from the capillary suspensions than for those made from the binary reference pastes. This demonstrates that the benefit of adding a secondary liquid to the wet paste with respect to the electrical conductivity is more pronounced at a higher polymer fraction in the dry film. For the system investigated here, an increase in electrical conductivity of 135 ± 8% could be achieved for films including 70 wt.% resin in the continuous phase of the wet paste.

These findings further support the hypothesis that the higher conductivity in films made from capillary suspensions is achieved when the secondary liquid keeps the particle contact points free from the polymer and that this is particularly helpful at higher polymer content in the film. The data obtained for the low boiling secondary fluid demonstrate that the formation of the capillary suspension network structure in the wet paste itself is not sufficient to achieve an enhanced conductivity at high particle loadings well above the percolation threshold. This hypothesis will be further discussed in the following section based on SEM imaging.

3.3. SEM Imaging of Particle–Particle Contact Area

To understand the changes observed in electrical conductivity, the particle contact areas were investigated with high magnification SEM imaging. Figure 7 depicts polymer shells observed in the sputtered broken samples, which can be assumed to originate from particles that were pulled out during the preparation process. These shells show only minimal changes due to the release of particles during fracture, and therefore provide insight into how the particles were embedded in the polymer matrix prior to preparation. All depicted samples exhibit the same polymer content of 40 wt.% in the continuous phase, but were prepared from pastes including secondary liquids with different boiling ranges.

In the reference sample without secondary liquid (Figure 7a), particle imprints surrounded by polymer shells can be observed, through which the underlying particle appears

faintly bright. Despite this transparency, the polymer shells remain fully intact, indicating that the polymer fully wets and covers the particle–particle contact regions. The same behavior can be observed with the low boiling secondary liquid (Figure 7b); as it leaves the sample before the solvent evaporates and the epoxy resin cures, it allows the resin sufficient time to flow back into the particle–particle contact regions. Accordingly, the electrical conductivity is the same as for the binary reference system. In contrast, samples containing medium boiling and high boiling secondary liquids frequently exhibit almost circular holes in the residual particle shells through which the underlying particles are clearly visible (see Figure 7c,d, highlighted by red arrows). These holes are presumably created due to the presence of the secondary liquid in the contact regions during drying and curing of the epoxy solution. To quantify this phenomenon, the total number of visible polymer shells left behind by particles during breaking as well as those exhibiting a characteristic hole was counted for each SEM image (see Figure 7e). While no holes, or at most one random hole, were observed in the reference sample and the sample resulting from the paste including the low boiling secondary fluid, a significantly higher number of polymer shells with holes was found in the samples prepared from pastes including medium boiling and high boiling secondary fluids, corresponding to approximately 60% of the polymer shells exhibiting a characteristic hole. A more comprehensive statistical analysis, including hole size distributions and the systematic evaluation and comparison of different sample regions, will be pursued in future work. These polymer-depleted particle–particle contact regions provide a plausible explanation for the observed substantial increase in electrical conductivity when the medium boiling secondary liquid is present. For the films made from pastes including the high boiling secondary liquid, however, the electrical conductivity is substantially lower than for those made from pastes including the medium boiling secondary liquid, and at lower drying temperature the conductivity is even lower than that of the reference without secondary liquid. We attribute these effects to remnants of the high boiling secondary liquid in the contact zones, acting as an insulator.

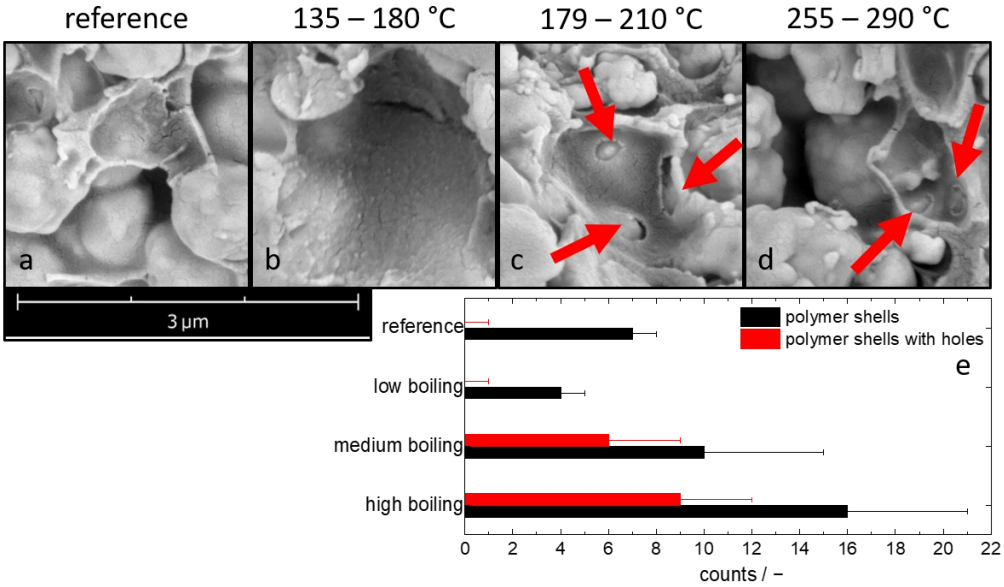

Figure 7. SEM images of polymer shells left by pulled out particles on the fracture surface of composite films obtained from pastes with 40 vol% silver particles and 40 wt.% epoxy resin in the continuous phase (**a**) without a secondary liquid in the wet paste, and (**b**–**d**) prepared with secondary liquids with rising boiling range. (**b**) Prepared from wet pastes with ϕ_{sec}/ϕ_{sol} = 0.2 due to not forming a stable network at lower contents (**c**,**d**) with ϕ_{sec}/ϕ_{sol} = 0.1. (**e**) Statistic of total counted polymer shells (black) and shells with holes (red) per image. Samples were dried at 150 °C for 10 min; red arrows are to guide the eye.

To gain deeper insights, images were taken at higher polymer concentrations, where the increase in conductivity due to the presence of the medium boiling secondary liquid was even more pronounced. Figure 8 shows SEM images of samples with higher polymer content made from pastes including low boiling and medium boiling secondary liquids. In the reference without a secondary liquid, intact polymer shells are consistently observed across all characterized samples, independent of polymer content (see Figures 7a and 8a,d). In the same way, for samples made from pastes including the medium boiling secondary liquid, circular holes in the polymer shells are always found irrespective of polymer concentration (see Figures 7c and 8c,f). In samples with the low boiling secondary liquid, a change in the polymer content can be observed. For films made from the pastes with 40 wt.% (Figure 7b) and 60 wt.% (Figure 7b) epoxy resin in the continuous phase, no circular holes in the polymer shells could be observed, and accordingly the conductivity is similar as for the samples made from the binary paste (see Figure 6b). At a polymer content of 80 wt.%, however, holes in the polymer shells occur frequently (see Figure 8e). This is in line with the observed 37 ± 4% increase in conductivity compared to the corresponding sample made from the binary paste. On the other hand, the conductivity is still about four times lower than that of the film made from the paste including the medium boiling secondary liquid. These results suggest that part of the low boiling secondary liquid evaporates fast enough to allow for a penetration of polymer into the contact regions, thus fewer polymer-free particle–particle contacts are available than in the system including the medium boiling secondary liquid.

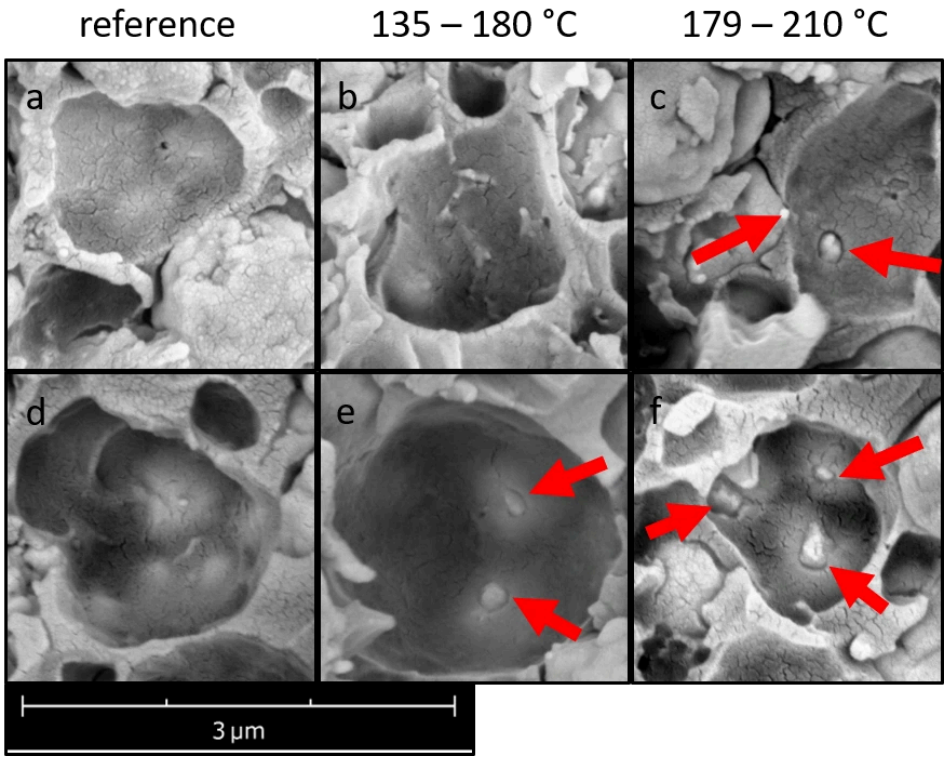

Figure 8. SEM images of polymer shells left by pulled out particles on the fracture surface of composite films obtained from pastes with 40 vol% silver as well as 60 wt.% (**a**–**c**) and 80 wt.% (**d**–**f**) epoxy resin in the continuous phase, respectively, (**a**,**d**) without secondary liquid in the wet paste, (**b**,**e**) with the low boiling secondary liquid at ϕ_{sec}/ϕ_{sol} = 0.2, and (**c**,**f**) with the medium boiling secondary liquid at ϕ_{sec}/ϕ_{sol} = 0.1. Samples were dried at 150 °C for 10 min; red arrows are to guide the eye.

3.4. Transfer of the Concept to a Thermoplastic System

Thermoplastic polymers are also widely used as matrix material for conductive composites. To verify whether the concept of keeping a secondary liquid in the contact zone during solidification of a polymer composite film is applicable to other systems, it was transferred to a model system utilizing the thermoplastic polymer polyvinyl acetate (PVAc), while the same solvent and particles as described above were used. For demonstration purposes, only the effect of the medium boiling secondary liquid was investigated. As mentioned previously, the formation of a capillary suspension was first assessed using the increase in the yield stress as an indicator.

At a silver fraction of 40 vol.% and a ratio of secondary liquid to particle volume fraction of 0.1, a yield stress of about 150 Pa is observed, which is about twice as high as that of the corresponding binary system, thus clearly indicating the formation of a capillary suspension. A similar increase in yield stress was found for other samples including different amounts of polymer, thus clearly indicating the formation of a capillary suspension.

In Figure 9, the electrical conductivity of films made from the pastes described above is plotted as a function of the polymer content in the primary liquid. For the highest polymer content, a two-phase reference sample without secondary fluid was also prepared and measured for comparison.

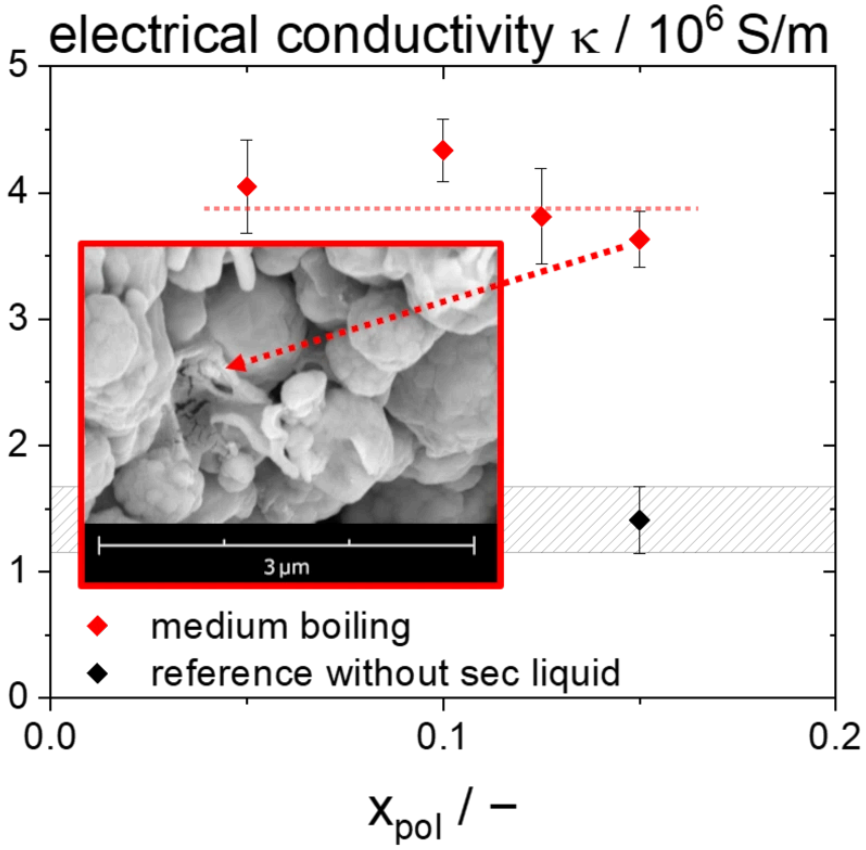

Figure 9. Electrical conductivity of films made from capillary suspensions including 40 vol% spherical silver particles as conductive fillers, a medium boiling secondary liquid with $\phi_{sec}/\phi_{sol} = 0.1$, and a solution of the thermoplastic polymer PVAc in benzyl alcohol as primary liquid phase as a function of the polymer content in this continuous phase (red symbols). Conductivity of a film made from a paste without secondary liquid is shown as reference (black symbol). Samples were dried for 10 min at 200 °C. The inserted SEM image depicts a polymer shell left by pulled out particles prepared from a paste with 15 wt.% polymer in the continuous phase. Lines and arrows are to guide the eye.

All samples made from ternary pastes exhibit an electrical conductivity κ in the range of 4×10^6 S/m, irrespective of polymer content. This is more than twice as high as the conductivity of the film made from the binary paste. Since the presence of capillary bridges between the particles depends only on the ratio of secondary liquid to particles, and not on the polymer content in the paste, the corresponding holes in the particle contact regions remain unchanged. Variations in polymer content affect the areas outside these regions and thus have no effect on conductivity. Corresponding SEM images of the fracture surfaces of films made from pastes including a medium boiling secondary liquid again show holes in the polymer shells around pulled out particles, as exemplarily shown as an insert in Figure 9 for the film made from the wet paste including 15 wt.% polymer in the continuous phase. The presence of these holes indicates the possibility of facilitated electron transport, which may explain the increased conductivity observed in samples with polymer-free contact regions. By transferring the method of creating polymer-free contacts via capillary suspensions to another matrix system, these results further support the hypothesis that this concept can be generically used to deposit a volatile component at the particle contact regions to keep these areas free of polymer during drying and solidification of the polymer phase, thus significantly enhancing the electrical conductivity of polymer composites including conductive fillers.

4. Conclusions

The presented work introduces the capillary suspension concept as an alternative to conventional two-phase filler/polymer systems for the formulation of highly conductive polymer composites. Previously, there was little or no conductivity improvement in highly filled composites well above the percolation threshold. In such systems, many particle contacts already exist due to geometrical constraints, and the presence of a secondary liquid per se does not improve that significantly.

Here, we have demonstrated that this limitation can be overcome. We have extended the capillary suspension concept through a targeted selection of the secondary liquid. Delaying the evaporation of the secondary liquid until the polymer in the continuous phase is immobilized provides polymer-free particle–particle contact regions, and thus leads to a substantially enhanced electrical conductivity in highly filled systems.

The effectiveness of this strategy is first demonstrated using a thermosetting system with secondary liquids of varying boiling ranges. First, it was shown that a particle network stabilized by capillary forces could be created with these secondary liquids using the increase in yield stress due to secondary liquid addition as an indicator. The resulting stabilized particle network can be transferred to the dried, cured polymer composite, as demonstrated by SEM images of fractured sample surfaces.

Adding the medium boiling secondary liquid yielded an about two-fold increase in electrical conductivity in films dried at 200 °C corresponding to the boiling temperature range of this solvent mixture, and SEM images clearly revealed frequently occurring polymer-free particle–particle contact regions.

No conductivity enhancement is found for the low boiling secondary liquid in films made from pastes including 40 wt.% and 60 wt.% polymer in the primary phase of the wet paste. In these cases, this additive evaporates too fast to keep the particle–particle contact zones free of polymer as confirmed by SEM images.

The high boiling secondary liquid does not yield an enhanced electrical conductivity in films dried at 150 °C, despite the polymer-free contact regions observed in SEM images. In these samples, the secondary liquid seems to remain in the contact regions acting as an insulating layer between the particles instead of the polymer. At 200 °C drying temperature, an increase in electrical conductivity is observed compared to the binary system, but this

increase is less pronounced than for the medium boiling additive, again suggesting that remnants of the high boiling secondary liquid in the contact zones act as an insulator.

Finally, the concept was successfully transferred to a system including a thermoplastic instead of a thermoset polymer and a more than two-fold increase in electrical conductivity was achieved in this case.

The concept of capillary suspensions thus is demonstrated to be a generic strategy to enhance the electrical conductivity of highly concentrated composite materials consisting of polymers and conductive fillers. Further studies should address the influence of particle shape and surface treatment on the resulting electrical conductivity. In addition, long-term stability and durability should be evaluated through standardized testing protocols, including thermocycling and damp heat exposure, complemented by a comprehensive mechanical characterization, particularly with respect to applications in PV technology. Particular attention should be given to a detailed statistical analysis of hole formation, including a thorough assessment of hole size distributions and their spatial variability within the samples. In addition, future work will systematically investigate the extent to which the observed phenomena can be applied to a broader range of application scenarios. The here characterized outstanding materials may find application in various fields of printed electronics, in particular as low-temperature metallization pastes for thermosensitive solar cells, such as heterojunction silicon or perovskite tandem cells.

5. Patents

Patents related to this work are listed below.

Abdel Aal K, Dyhr K, Ailinger M, Steck A-M, Willenbacher N. "Process for the preparation of a conductive polymer composite with increased conductivity, polymer composite obtained therefrom, and use of the conductive polymer composite with increased conductivity".

German Patent Application. 102025138381.2 (2025).

Author Contributions: K.D. and K.A.A. have contributed equally. Conceptualization, K.D. and K.A.A.; methodology, K.D. and K.A.A.; validation, K.D., K.A.A. and A.-M.S.; formal analysis, K.D. and K.A.A.; investigation, K.D. and K.A.A.; resources, N.W.; data curation, K.D., K.A.A. and A.-M.S.; writing—original draft preparation, K.D. and K.A.A.; writing—review and editing, K.D., K.A.A. and N.W.; visualization, K.D. and K.A.A.; supervision, N.W.; project administration, N.W.; funding acquisition, N.W. All authors have read and agreed to the published version of the manuscript.

Funding: This research received no external funding.

Data Availability Statement: The raw data supporting the conclusions of this article will be made available by the authors on request.

Acknowledgments: The authors acknowledge Thomas Lebe (Karlsruhe Institute of Technology, Institute of Mechanical Process Engineering and Mechanics) for assistance with scanning electron microscopy imaging and Klara Urbschat (Karlsruhe Institute of Technology, Institute for Chemical Technology and Polymer Chemistry) for assistance with DSC and TGA measurements. The authors also thank Aurelia Kuhn for assistance with experimental work.

Conflicts of Interest: The authors declare no conflicts of interest.

Abbreviations

The following abbreviations are used in this manuscript:

ECA	Electrically Conductive Adhesive
SEM	Scanning Electron Microscope
PVP	Polyvinylpyrrolidone

PERC	Passivated Emitter and Rear Cell
ITRPV	International Technology Roadmap for Photovoltaics

References

1. Wiklund, J.; Karakoç, A.; Palko, T.; Yiğitler, H.; Ruttik, K.; Jäntti, R.; Paltakari, J. A Review on Printed Electronics: Fabrication Methods, Inks, Substrates, Applications and Environmental Impacts. *J. Manuf. Mater. Process.* **2021**, *5*, 89. [CrossRef]
2. Baldé, C.P.; Kuehr, R.; Yamamoto, T.; McDonald, R.; D'Angelo, E.; Althaf, S.; Bel, G.; Deubzer, O.; Fernandez-Cubillo, E.; Forti, V.; et al. *Global E-Waste Monitor 2024*; International Telecommunication Union (ITU) and United Nations Institute for Training and Research (UNITAR): Geneva/Bonn, Switzerland, 2024.
3. Lossen, J.; Matusovsky, M.; Noy, A.; Maier, C.; Bähr, M. Pattern Transfer Printing (PTP^{TM}) for c-Si Solar Cell Metallization. *Energy Procedia* **2015**, *67*, 156–162. [CrossRef]
4. Martins, P.; Pereira, N.; Lima, A.C.; Garcia, A.; Mendes-Filipe, C.; Policia, R.; Correia, V.; Lanceros-Mendez, S. Advances in Printing and Electronics: From Engagement to Commitment. *Adv. Funct. Mater.* **2023**, *33*, 2213744. [CrossRef]
5. Rao, C.H.; Avinash, K.; Varaprasad, B.K.S.V.L.; Goel, S. A Review on Printed Electronics with Digital 3D Printing: Fabrication Techniques, Materials, Challenges and Future Opportunities. *J. Electron. Mater.* **2022**, *51*, 2747–2765. [CrossRef]
6. Wu, W. *Printed Electronics Technologies*; The Royal Society of Chemistry: Cambridge, UK, 2022.
7. Tepner, S.; Lorenz, A. Printing Technologies for Silicon Solar Cell Metallization: A Comprehensive Review. *Prog. Photovolt. Res. Appl.* **2023**, *31*, 557–590. [CrossRef]
8. Ballif, C.; Huljić, D.M.; Willeke, G.; Hessler-Wyser, A. Silver Thick-Film Contacts on Highly Doped *n*-Type Silicon Emitters: Structural and Electronic Properties of the Interface. *Appl. Phys. Lett.* **2003**, *82*, 1878–1880. [CrossRef]
9. Chen, D.; Chen, Y.; Wang, Z.; Gong, J.; Liu, C.; Zou, Y.; He, Y.; Wang, Y.; Yuan, L.; Lin, W.; et al. 24.58% Total Area Efficiency of Screen-Printed, Large Area Industrial Silicon Solar Cells with the tunnel Oxide Passivated Contacts (i-TOPCon) Design. *Sol. Energy Mater. Sol. Cells* **2020**, *206*, 110258. [CrossRef]
10. Jiang, J.; He, Y.; Zhang, Z.; Wei, J.; Li, L. Pb-free front-contact silver pastes with SnO-P_2O_5 glass frit for crystalline silicon solar cells. *J. Alloys Compd.* **2016**, *689*, 662–668. [CrossRef]
11. Dong, Y.; Chen, L.; Mao, H.; Yang, H. High-Performance Low-Temperature Silver Paste Used for Silicon Heterojunction Solar Cells Through Material Selection and Formulation Optimization. *J. Electron. Mater.* **2025**, *54*, 4606–4617. [CrossRef]
12. Scenev, V.; Szalapak, J.; Werft, L.; Hoelck, O.; Jakubowska, M.; von Krshiwoblozki, M.; Kallmayer, C.; Schneider-Ramelow, M. Low-Temperature Processible Highly Conducting Pastes for Printed Electronics Applications. *Adv. Eng. Mater.* **2022**, *24*, 2101752. [CrossRef]
13. Li, D.; Yuan, J.; Chu, L.; Shen, L.; Huang, Z.; Zhang, L.; Bao, N. Overcoming the Trade-off Between Curing Temperature and Conductivity for High-Performance Conductive Silver Pastes. *Front. Mater. Sci.* **2025**, *19*, 250733. [CrossRef]
14. Santamaria, A.; Muñoz, M.E.; Fernández, M.; Landa, M. Electrically Conductive Adhesives with a Focus on Adhesives that Contain Carbon Nanotubes. *J. Appl. Polym. Sci.* **2013**, *129*, 1643–1652. [CrossRef]
15. Aradhana, R.; Mohanty, S.; Nayak, S.K. A Review on Epoxy-Based Electrically Conductive Adhesives. *Int. J. Adhes. Adhes.* **2020**, *99*, 102596. [CrossRef]
16. Sorokin, A.E.; Sagomonova, V.A.; Petrova, A.P.; Solov'yanchik, L.V. Thermoplastic-Based Binders for Polymer-Composite Materials (Literature Review). *Polym. Sci. Ser. D* **2022**, *15*, 359–365. [CrossRef]
17. Zeng, X.; He, P.; Hu, M.; Zhao, W.; Chen, H.; Liu, L.; Sun, J.; Yang, J. Copper Inks for Printed Electronics: A Review. *Nanoscale* **2022**, *14*, 16003–16032. [CrossRef] [PubMed]
18. Kamyshny, A.; Magdassi, S. Conductive Nanomaterials for Printed Electronics. *Small* **2014**, *10*, 3515–3535. [CrossRef] [PubMed]
19. Hallam, B.; Kim, M.; Zhang, Y.; Wang, L.; Lennon, A.; Verlinden, P.; Altermatt, P.P.; Dias, P.R. The Silver Learning Curve for Photovoltaics and Projected Silver Demand for Net-Zero Emissions by 2050. *Prog. Photovolt. Res. Appl.* **2023**, *31*, 598–606. [CrossRef]
20. Newman, P.; Meader, N.; Klapwijk, P.; Chou, E.; Gao, Y.; Barot, H.; Yau, S.; Liang, J.; Smith, J.; Diwe, A.; et al. *World Silver Survey 2025*; The Silver Institute: Washington, DC, USA, 2025.
21. Karásek, L.; Meissner, B.; Asai, S.; Sumita, M. Percolation Concept: Polymer-Filler Gel Formation, Electrical Conductivity and Dynamic Electrical Properties of Carbon-Black-Filled Rubbers. *Polym. J.* **1996**, *28*, 121–126. [CrossRef]
22. Lyons, A.M. Electrically Conductive Adhesives: Effect of Particle Composition and Size Distribution. *Polym. Eng. Sci.* **1991**, *31*, 445–450. [CrossRef]
23. van Impelen, D.; Perius, D.; González-García, L.; Kraus, T. The Importance of Shape: Flakes and Spheres in Recyclable Conductive Pastes for Printed Electronics. *RSC Sustain.* **2025**, *3*, 1800–1806. [CrossRef]
24. Kirscht, T.; Bera, A.; Marander, M.; Grota, C.; Liu, F.; Jiang, S. Smaller is Better: Reducing Silver Nanoparticle Size Without Excess Ligands Enhances Conductivity and Flexibility in Printed Thin Films. *npj Flex. Electron.* **2025**, *9*, 113. [CrossRef]

25. Seo, M.; Kim, J.S.; Lee, J.G.; Kim, S.B.; Koo, S.M. The Effect of Silver Particle Size and Organic Stabilizers on the Conductivity of Silver Particulate Films in Thermal Sintering Processes. *Thin Solid Films* **2016**, *616*, 366–374. [CrossRef]
26. Shen, X.; Li, J.; Xi, S. High Strength Die-Attach Joint Formation by Pressureless Sintering of Organic Amine Modified Ag Nanoparticle Paste. *Nanomaterials* **2022**, *12*, 3351. [CrossRef] [PubMed]
27. Park, S.-H.; Hwang, J.; Park, G.-S.; Ha, J.-H.; Zhang, M.; Kim, D.; Yun, D.-J.; Lee, S.; Lee, S.H. Modeling the Electrical Resistivity of Polymer Composites with Segregated Structures. *Nat. Commun.* **2019**, *10*, 2537. [CrossRef] [PubMed]
28. Tian, K.; Jing, J.; Wen, M.; Zhang, L.; Li, Q.; Cheng, M.; Wen, J.; Wen, Y.; Wen, Y.; Fu, Q.; et al. Designing Functional Filler Networks via In Situ Silver Nanoparticles Through Barrier Tuning and Volume Exclusion. *Nat. Commun.* **2025**, *17*, 728. [CrossRef] [PubMed]
29. Wei, H.; Luo, H.; Wang, L.; Gao, Q.; Chen, Y.; Xiang, J.; Fan, H. Lightweight and Self-Healing Thermally Expandable Microsphere/Silver Composites with Segregated Conductive Network for High-Efficiency Electromagnetic Interference Shielding. *J. Appl. Polym. Sci.* **2023**, *140*, e54662. [CrossRef]
30. Shida, K.; Sahara, R.; Tripathi, M.; Mizuseki, H.; Kawazoe, Y. Controlling the Percolation Threshold of Conductor-Insulator Composites by Changing the Granular Size of Insulators. *Mater. Trans.* **2010**, *51*, 1141–1144. [CrossRef]
31. Kronsbein, M.; Böck, L.; Rößler, T.; Willenbacher, N. Low-Filled Electrically Conductive Adhesives Based on Silver-Coated Glass and Copper Particles. *Sol. Energy Mater. Sol. Cells* **2026**, *299*, 114228. [CrossRef]
32. Zhang, H.; Mao, Z.; Zhang, J.; Zhang, Z.; Chabi, S.; Abidi, N. Melt-Processed Bi-Continuous Phase Polymer Composite with Selective Filler Localization: A Mini Review. *Polym. Rev.* **2024**, *64*, 1098–1135. [CrossRef]
33. Koos, E.; Willenbacher, N. Capillary Forces in Suspension Rheology. *Science* **2011**, *331*, 897–900. [CrossRef] [PubMed]
34. Sun, H.; Zhang, X.; Yuen, M.M. Enhanced Conductivity Induced by Attractive Capillary Force in Ternary Conductive Adhesive. *Compos. Sci. Technol.* **2016**, *137*, 109–117. [CrossRef]
35. Sun, H.; Han, Z.; Willenbacher, N. Ultrastretchable Conductive Elastomers with a Low Percolation Threshold for Printed Soft Electronics. *ACS Appl. Mater. Interfaces* **2019**, *11*, 38092–38102. [CrossRef] [PubMed]
36. Abdel Aal, K.; Dyhr, K.; Ailinger, M.; Steck, A.-M.; Willenbacher, N. *Verfahren Zur Herstellung Eines Leitfähigen Polymerkomposits Mit Erhöhter Leitfähigkeit, Daraus Erhaltenes Polymerkomposit Und Verwendung Des Leitfähigen Polymerkomposits Mit Erhöhter Leitfähigkeit*; German Patent and Trade Mark Office: Munich, Germany, 2025.
37. Larsson, M.; Duffy, J. An Overview of Measurement Techniques for Determination of Yield Stress. *Annu. Trans. Nord. Rheol. Soc.* **2013**, *21*, 125–138.
38. Dinkgreve, M.; Paredes, J.; Denn, M.M.; Bonn, D. On Different Ways of Measuring "the" Yield Stress. *J. Non-Newton. Fluid Mech.* **2016**, *238*, 233–241. [CrossRef]
39. *DIN EN ISO 19403*; Paints and Varnishes—Wettability. ISO: Geneva, Switzerland, 2023.
40. *ASTM D2240*; Test Method for Rubber PropertyDurometer Hardness. ASTM: West Conshohocken, PA, USA, 2021.
41. Schneider, M.; Maurath, J.; Fischer, S.B.; Weiß, M.; Willenbacher, N.; Koos, E. Suppressing Crack Formation in Particulate Systems by Utilizing Capillary Forces. *ACS Appl. Mater. Interfaces* **2017**, *9*, 11095–11105. [CrossRef] [PubMed]
42. Fischer, S.B.; Koos, E. Influence of Drying Conditions on the Stress and Weight Development of Capillary Suspensions. *J. Am. Ceram. Soc.* **2021**, *104*, 1255–1270. [CrossRef]